Progress in Physics of Applied Materials 2 (2022) 133–138

Semnan University

Progress in Physics of Applied Materials

journal homepage: https://ppam.semnan.ac.ir/

# Improving performance and stability of silver bismuth iodide solar cells using carbon nanotubes in the hole transport layer

**S.S. Hosseini, M. Adelifard***

*School of Physics, Damghan University, Damghan, Iran*

**ARTICLE INFO**

Article history:
Received: 15 November 2022
Revised: 29 November 2022
Accepted: 17 December 2022

Keywords:
Photovoltaic
Lead-free
Perovskite solar cells
Silver bismuth iodide
CNT

**ABSTRACT**

Silver bismuth iodide (SBI) materials are low-toxic, air-stable, and suitable for replacing lead-based perovskite ones. In this work, the photovoltaic characteristics of SBI-based solar cells with different hole transport layers (HTL) were investigated. Results showed that the power conversion energy (PCE) of Silver bismuth iodide-based solar cells with P3HT as HTL was higher than spiro-OMeTAD. Also, the influence of CNT as a dopant on the performance and stability of the devices was studied. CNT doping of silver bismuth iodide increased the Voc and so the efficiency of the solar cell was enhanced. Furthermore, Also, CNT-doped P3HT improves the interface contact between the active layer and HTL and increases the conductivity of HTL. The best PCE of about 2.16% for devices with FTO/c-$TiO_2$/m-$TiO_2$/silver bismuth iodide-CNT/P3HT-CNT/Au structure was obtained. Moreover, the stability of solar cells under environmental conditions after 30 days was investigated. All devices preserved about 95% of their efficiency.

## 1. Introduction

One of the most important photovoltaic devices is the lead-based perovskite solar cell (PSC). Despite the rapidly advance in the efficiency of over 25%, instability of solar cells and toxicity of lead impacted the commercialization of these devices. This has led to search for alternatives to lead [1-7].

Most Pb-free perovskite light absorbers are based on Tin (Sn), Germanium (Ge), and bismuth (Bi). Sn is toxic and also Sn and Ge based devices have poorer stability than Pb because of the simple oxidation of $Sn^{2+}$ to $Sn^{4+}$ and $Ge^{2+}$ to $Ge^{4+}$. Bi based devices have attracted great attention because they are low toxic and more stable than lead. Trivalent bismuth ($Bi^{3+}$) has a lone pair of $6s^2$ electrons (isoelectronicity with $Pb^{2+}$) and because of high born effective charges, these lone pair cations could have high dielectric constants. Also, it has similar ionic radius to $Pb^{2+}$, great absorption coefficient, and high carrier diffusion life time. However, they have lower PCE compared with Pb based devices because of their surface morphology and relatively high bandgap energies (>2 eV) [7, 8].

Silver bismuth iodide (SBI) compounds with $Ag_aBi_bI_{a+3b}$ formula (rudorffites) have attracted considerable attention because of their electrical and optical properties. They are semiconductors with direct bandgaps of below 2 eV and also air stable [9-17].

For the first time in 2016, Kim et al. [9] used a solution-based method to prepare solar cells based on $AgBi_2I_7$. They estimated bandgap energy of 1.87 eV for $AgBi_2I_7$ and PCE of 1.2%. Also, they showed that this photovoltaic device is stable for 10 days under ambient conditions. Zhu et al. [10] fabricated silver-bismuth-iodide with different ratios of $AgI/BiI_3$ for use in solar cells. They obtained indirect and direct band gap energies of 1.62 eV and 1.85 eV, respectively. They obtained a PCE of 2.1%. Turkeych et al. [11] demonstrated a PCE of 4.3% for device with $Ag_3BiI_6$ as light absorber. They fabricated the $AgBiI_4$, $Ag_2BiI_5$, $Ag_3BiI_6$, and $AgBi_2I_7$ thin films with the direct band gap energy values in the range of 1.79-1.83 eV. Jung et al. [12] demonstrated the best PCE of 2.31% for devices based on $Ag_2BiI_5$ with a hexagonal structure, and the bandgap energy between 1.83 eV and 1.88 eV. Moreover, they indicated the stability of their devices after 30 days under ambient conditions. Shao et al. [13] compared three devices with no ETL, and with $TiO_2$ and $SnO_2$ as ETL and displayed that solar cells with $SnO_2$ as ETL had the best PCE of about 0.67%. Shao et al. [14] reported the best PCE of 0.83% for solar cells

* Corresponding author. Tel.: +98-9155198362
*E-mail address:* adelifard@du.ac.ir

DOI: 10.22075/PPAM.2022.28988.1040

based on rough $AgBi_2I_7$ films. Ghosh et al. [15] reported a PCE of 2.6% for the solar cells based on $Ag_2BiI_5$ deposited by a dynamic hot casting method. Pai et al. [16] used silver bismuth sulfoiodides as a light absorber in solar cells and achieved a PCE of 5.5%. Khazaee et al. [17] reported a two-step co-evaporation/ annealing method for depositing the silver bismuth iodide compositions. They presented the best PCE of 0.89% for $AgBiI_4$ based solar cells.

As can be seen in the above mentioned literatures, compare with lead-based thin film, silver bismuth iodide film has higher bandgap, and SBI solar cells have low short-circuit current ($J_{sc}$), open-circuit voltage ($V_{oc}$) and also low efficiency. In general, the $V_{oc}$ for SBI based devices are lower than that for lead based ones and are usually below 1 V. So, to improve the performance of the solar cells, the morphological and optical properties of SBI based devices should be corrected.

We have previously reported the influence of multi-walled carbon nanotube (MWCNT) as a dopant on the physical properties of SBI based solar cells [18]. We showed improvement in surface morphology of the SBI layers in presence of MWCNT and also they had the bandgap values in the range of 1.85-1.92 eV. Studies on the photovoltaic performance of devices demonstrated that compare with the pure silver bismuth iodide based samples with PCE of 0.44%, doping of MWCNT increased the PCE to 1.61% [18]. Furthermore, hole transport layer (HTL) of these devices is usually dopant-free. So, low $J_{sc}$ and efficiency could be related to the low conductivity of HTL. CNTs are often used as ETL and HTL in perovskite solar cells [19-28]. They increase conductivity and lead to higher $J_{sc}$ values. Also, they reduce trap centers and improve the perovskite surface and results higher $V_{oc}$. Furthermore, CNT-doped devices are highly stable. In addition, CNTs have unique optical and electrical properties. They are semiconductor materials with bandgap energy of below 1 eV and have absorption edges over 800 nm [19-28]. To achieve these goals, in the present work we tried to improve photovoltaic properties of SBI based devices. At first we compared dopant-free spiro and P3HT as HTL. Then the effect of the carbon nanotube (CNT) as a dopant in hole transport layer was investigated.

## 2. Experimental details

### *2.1. Materials*

In this research, BiI3 (99.9%, Aldrich), AgI (99.9%, Aldrich), MWCNT (>95%, US Nano), were used as the precursors. 2, 2', 7, 7'-Tetrakis (N,N-di-p-methoxy phenylamino)-9,9'-spirobifluorene (spiro-OMeTAD, >99.5%, Luminescence Technology Corp) and poly(3-hexylthiophene-2,5-diyl) (P3HT, >99.5%, Luminescence Technology Corp) were used as hole transport materials and chlorobenzene (99.8%, Sigma-aldrich) was used as solvent.

### *2.2. Fabrication of Solar Cells*

We employed direct mesoporous architecture for the fabrication of the FTO/c-$TiO_2$/m-$TiO_2$/Absorber/HTL/Au photovoltaic cell. We used silver bismuth iodide compound with molar ratios of $AgI/BiI_3$=2 (SBI) and SBI+0.3wt%CNT (SBI-C) as light absorber layer, also, spiro-OMeTAD, P3HT, and P3HT+0.05wt%CNT (P3HT-C) as hole transport layers. All devices were fabricated as described in our previous report [19].

To prepare the hole transport layer, (i) 72.3 mg of spiro-OMeTAD was dissolved in 1 mL of chlorobenzene and 30 µL of this solution was spin-coated at 4000 rpm for 30 s, or (ii) 15 mg of P3HT (or P3HT+0.05Wt%CNT) was dissolved in 1 mL of chlorobenzene and 30 µL of this solution was spin-coated at 2000 rpm for 1 min. Finally, Au electrode was evaporated on top of the HTL. The Schematic image of the final device is demonstrated in Figure 1.

### *2.3. Characterization*

X-ray diffraction (XRD) patterns were recorded on an X-ray diffractometer (Bruker-AXS D8 Advance Cu-Kα). The morphologies of the studied layers and the amount of different elements were detected by a field emission scanning electron microscope and energy dispersive X-ray spectroscopy (FE-SEM and EDX, TESCAN MIRA3), respectively. Optical data was measured by UV–Vis Spectrophotometer (Model UNICO 4802) between 400 and 1100 nm. Current density–voltage (*J*–*V*) measurement was recorded by a solar simulator under the standard AM 1.5G situation (100 mW $cm^{-2}$).

## 3. Results and discussion

### *3.1. XRD patterns*

Fig. 2 shows XRD patterns of SBI and SBI-C layers on the top of the FTO/cp-TiO2/mp-TiO2 structure. The peaks appeared at 2θ values about 12.8°, 23.8°, 25.2°, 26.3°, and 29.2° show that the main phase is the hexagonal phase of Ag2BiI5 with $R\bar{3}m$ space group symmetry corresponds to JCPDS card No.: 00-035-1025. In addition, other peaks refered to FTO (JCPDS card No.: 01-046-1088) were located at 2θ values of 33.8°, and 37.9° in the XRD patterns.

By studying the XRD patterns of the SBI and SBI-C samples, it was found that after adding CNT, the intensity of peaks decreased. Also, Due to the small amount of CNT, no peak is observed for it.

### *3.2. Morphological studies*

the prepared thin films were studied using FESEM analysis. Fig. 3 shows top-view FESEM images of SBI (a,b) and SBI-C (c,d) active layers on top of the FTO/cp-$TiO_2$/mp-$TiO_2$ structure. As can be seen, the surface of pure SBI sample is covered by separated small particles. After doping, it seems that the morphology of the SBI thin film improves, and particle size is increased. CNT causes films with more compact surface and act as connector of the nanoparticles to each other. The thickness of the different layers is obvious in cross-sectional image of FTO/c-$TiO_2$/m-$TiO_2$/ SBI /P3HT/Au structure in Fig. 3-e. It can be seen that the thickness of the c-$TiO_2$, m-$TiO_2$+SBI, SBI, P3HT and Au layers is about 40 nm, 230 nm, 210 nm, 80 nm, and 110 nm, respectively.

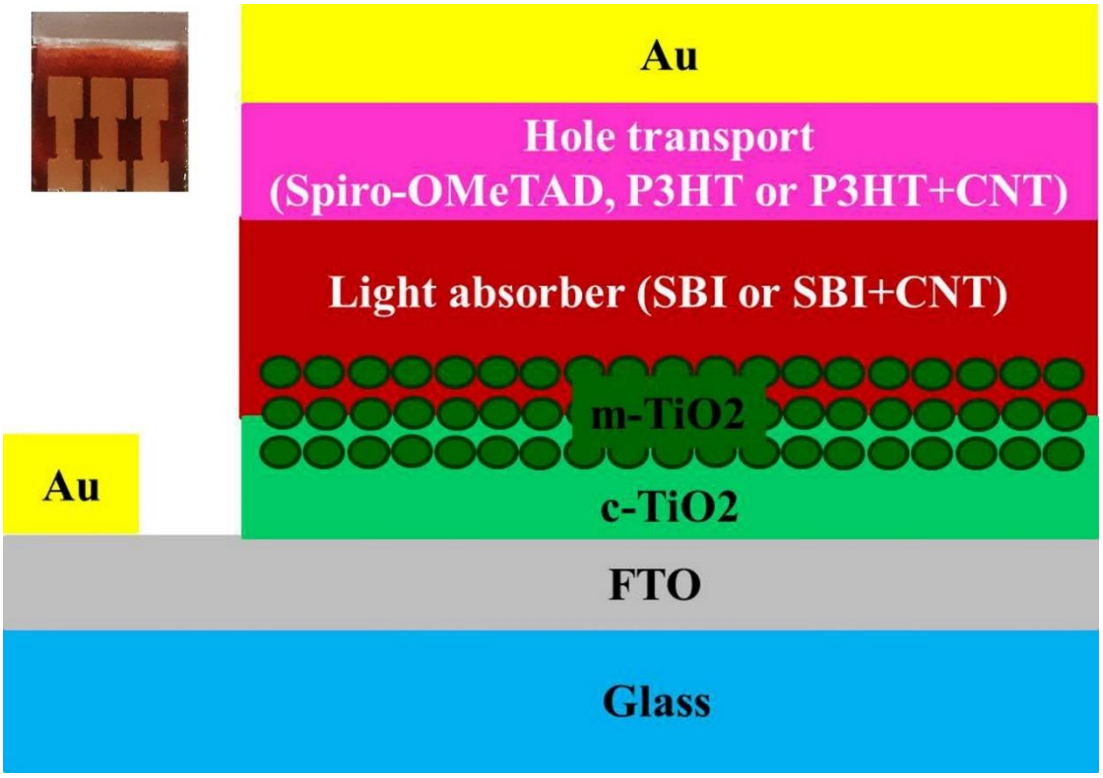


**Fig. 1.** Schematic and real images of the final device.

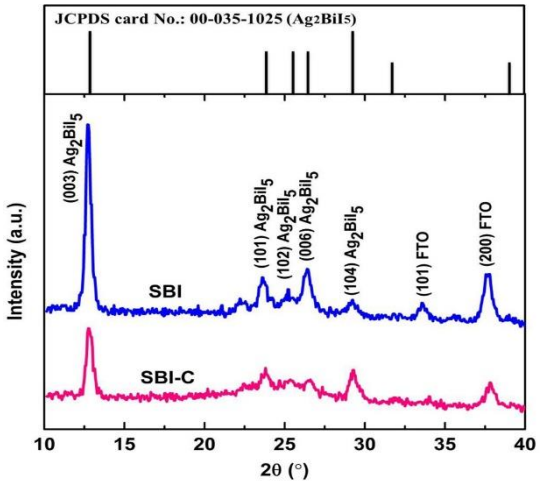


**Fig. 2.** XRD patterns of SBI and SBI+CNT samples.

### 3.3. Optical studies

The variations of the absorbance (A), versus wavelength for the prepared active layers, are presented in Figure 4 (a). The results show that the absorption edge of SBI-C thin film shifts to a higher wavelengths (λ~680nm) in comparison to pure SBI (λ~650 nm). This behavior is in agreement with the bandgap calculations. The details for the direct bandgap of these active layers are shown in Fig. 4 (b). According to curves, SBI film has a direct bandgap energy value of about 1.90 eV, and for SBI-C thin film, the bandgap value decreases to 1.82 eV. Shape, size, size distribution, phase, crystalline degree, and defects can play a role in the energy gaps of materials. Generally, $E_g$ becomes narrower by using larger particles in accordance with FESEM image of SBI-C, Fig. 3 (d).

### 3.4. Device results

Fig. 5 (a) shows forward bias sweep for the solar cells under simulated 1 sun irradiation, 100 mW cm$^{-2}$ intensity and standard air-mass 1.5 global spectrum. The short-circuit current ($J_{sc}$), open-circuit voltage ($V_{oc}$), fill factor (FF), series resistance ($R_S$), shunt resistance ($R_{Sh}$), and power conversion efficiency (PCE) derived from J-V curves are summarized in Table 1. It can be seen that compared with Spiro-OMeTAD, SBI-based solar cell with P3HT as HTL has better photovoltaic parameters. $J_{sc}$, $V_{oc}$, and FF values ~~were~~ increased and the PCE obtained in these devices was about 0.44% and 1.39% for solar cells with Spiro-OMeTAD and P3HT, respectively. So we chose P3HT as HTL to keep working. In our previous work, we studied the effect of CNT as a dopant in SBI and we observed that compared with the pure SBI samples, they showed better performance. Based on those results, we decided to use SBI-C instead of SBI as absorber layer in structure of solar cells. According to J-V curves, efficiency of solar cells based on SBI-C as absorber layer and P3HT as HTL was enhanced and it has a PCE of about 1.88%. Doping CNT improved the SBI surface, reduced the strains and so increased the $V_{oc}$ value (from 0.46 V to 0.55 V), which could lead to increase efficiency of devices. Furthermore, the effect of CNT doped P3HT was investigated. Results showed that SBI-C-based

solar cells with P3HT-C as HTL had the best PCE of about 2.16%. Actually, CNT doping improves the interface contact between the active layer and HTL and increases the conductivity of HTL and so it causes an increase in $J_{sc}$ and

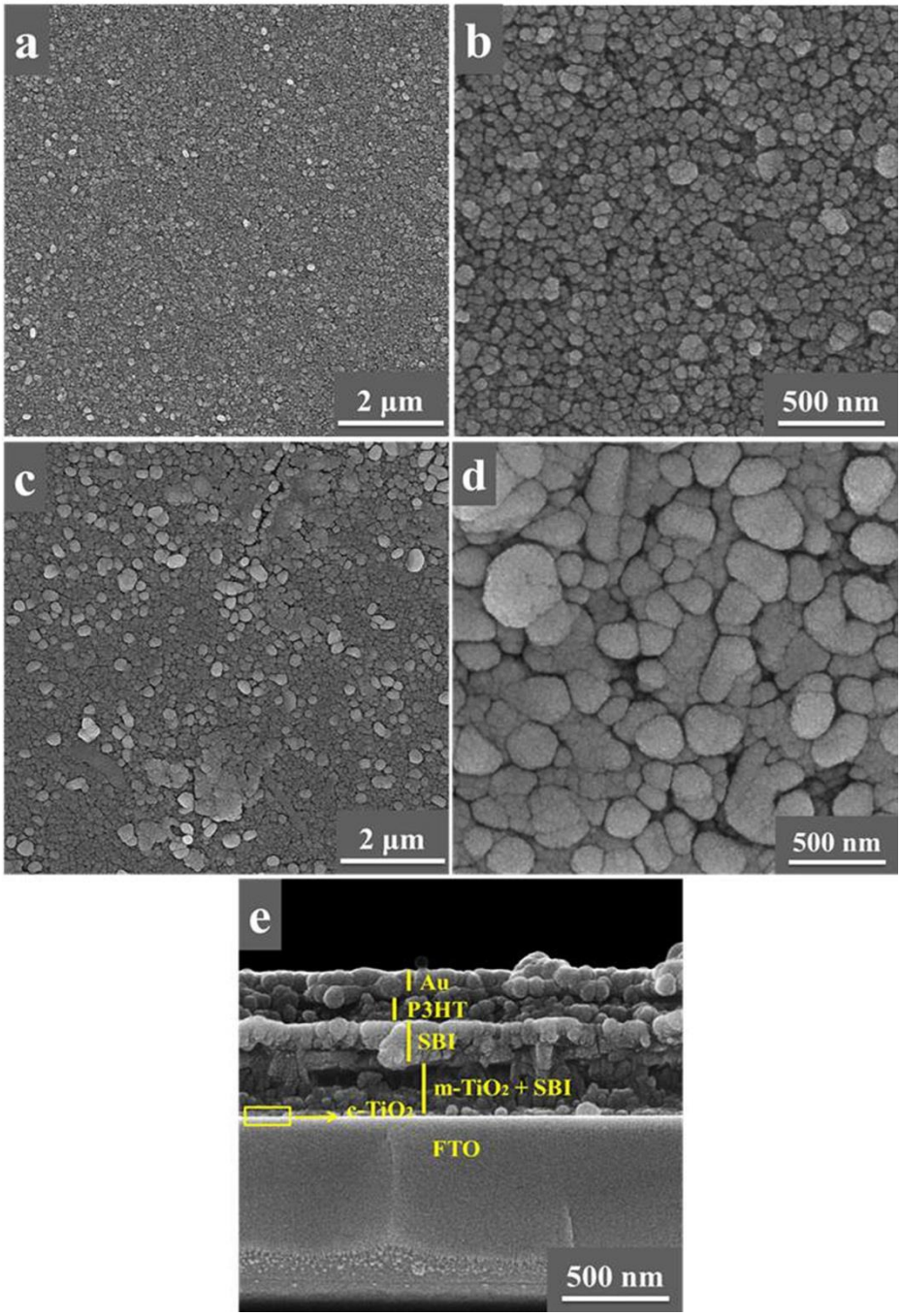


**Fig. 3.** Top-view FESEM images of (a,b) SBI (c,d) SBI+CNT sample, and (e) cross-sectional image of the FTO/cp-$TiO_2$/mp-$TiO_2$/SBI/P3HT/Au solar cell structure.

$V_{oc}$ (from $J_{sc}$=6.7 mA $cm^{-2}$ to 7.6 mA $cm^{-2}$ and $V_{oc}$=0.55 V to 0.58 V).

As it is known, the solar cells performance is affected by series and shunt resistances ($R_S$ and $R_{Sh}$). The $R_S$ is because of the resistance of the cell materials to current flow and shunt resistance is due to the leakage of current in cell. $R_S$ and $R_{Sh}$ have direct effect on fill factor. Increase in shunt resistance and decrease in series resistance causes higher fill factor and so better cell performance. From Table 1, it can be seen that the $R_S$ resistance is decreased and $R_{Sh}$ resistance is increased with using P3HT as HTL instead of Spiro-OMeTAD and Also use CNT as dopant. The results were in agreement with expectations and improved efficiency of devices.

Comparison of the photocurrent density versus voltage curves in both directions in Fig. 5 (b) shows low hysteresis of these solar cells so that both directions are almost the same.

Also, the stability of devices was investigated at 35 °C in 60% relative humidity. The PCE values for the solar cells after 30 days are mentioned in Table 1. Results show that CNT can increase the stability of SBI and P3HT. All devices were preserved more than 90% of their efficiency. However, the SBI-C-based device with P3HT-C as ETL

preserved about 98% of its efficiency and remains above 2.13%.

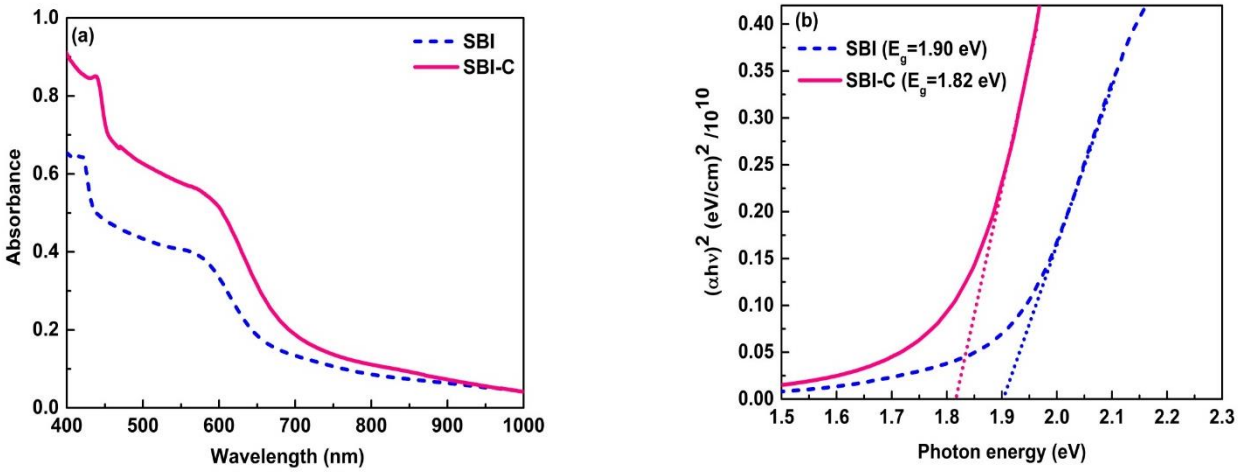


**Fig. 4.** (a) Absorption curves and (b) Optical band gap versus photon energy of SBI and SBI+CNT thin films.

**Table 1.** Photovoltaic parameters of solar cells.

| Sample | $V_{oc}$ (V) | $J_{sc}$ (mA cm$^{-2}$) | FF (%) | PCE (%) (0 day) | $R_S$ (Ω cm$^2$) | $R_{Sh}$ (Ω cm$^2$) | PCE (%) (30 day) |
|---|---|---|---|---|---|---|---|
| **SBI/Spiro** | 0.42±0.02 | 3.5±0.1 | 29.8±0.3 | 0.44±0.05 | 95.83 | 168.14 | 0.39±0.03 |
| **SBI/P3HT** | 0.46±0.04 | 6.5±0.2 | 46.6±0.4 | 1.39±0.03 | 36.88 | 169.69 | 1.28±0.01 |
| **SBI-C/P3HT** | 0.55±0.04 | 6.7±0.4 | 51.0±0.1 | 1.88±0.01 | 35.43 | 221.55 | 1.79±0.01 |
| **SBI-C/P3HT-C** | 0.58±0.04 | 7.6±0.1 | 49.0±0.1 | 2.16±0.01 | 33.89 | 174.67 | 2.13±0.02 |

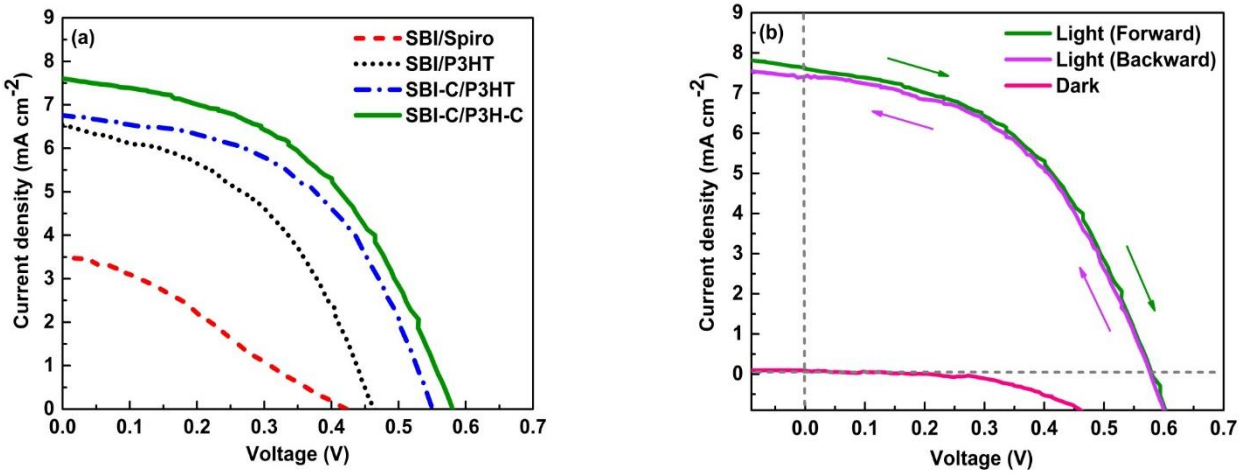


**Fig. 5.** (a) J–V characteristics and (b) comparison of the photocurrent density versus voltage curves in both directions of solar cells.

## 4. Conclusion

In summary, we have prepared SBI-based solar cells. Influence of CNT as dopants on performance and stability of devices was studied. The results demonstrated that PCE for SBI-based solar cell with P3HT as HTL was higher than that of spiro-OMeTAD. Furthermore, CNT doping of SBI increased the $V_{oc}$ and so efficiency of solar cell was enhanced. Also, CNT-doped P3HT improved the interface contact between the active layer and HTL and increases the conductivity of HTL and so it causes increase in $J_{sc}$ and $V_{oc}$ showed the best PCE of about 2.16% for devices with FTO/c-$TiO_2$/m-$TiO_2$/SBI-C/P3HT-C/Au structure.

Study on the stability of devices at 35 °C in 60% relative humidity for 30 days showed that CNT can increase the stability of devices. Although, all devices preserved more than 90% of their efficiency, the SBI-C-based device with P3HT-C as ETL preserved about 98% of its efficiency and remains above 2.13%.

## References

[1] A. Kojima, K. Teshima, Y. Shirai, and T. Miyasaka, Organometal halide perovskites as visible-light

sensitizers for photovoltaic cells. J. Am. Chem. Soc. 131(17), (2009) 6050.
[2] W.S. Yang, B.W. Park, E.H. Jung, N.J. Jeon, Y.C. Kim, D.U. Lee, and S.I. Seok, Iodide management in formamidinium-lead-halide–based perovskite layers for efficient solar cells. Science 356(6345), (2017) 1376.
[3] S.Z. Haider, H. Anwar, and M. Wang, Theoretical Device Engineering for High-Performance Perovskite Solar Cells Using CuSCN as Hole Transport Material Boost the Efficiency Above 25%. Phys. Status Solidi A 216(11), (2019) 1900102.
[4] C.F.J. Lau, Z. Wang, N. Sakai, J. Zheng, C.H. Liao, M. Green, S. Huang, H. J. Snaith, and A. Ho-Baillie, Fabrication of efficient and stable CsPbI3 perovskite solar cells through cation exchange process. Adv. Energy Mater. 9(36), (2019) 1901685.
[5] S. Ito, G. Mizuta, S. Kanaya, H. Kanda, T. Nishina, S. Nakashima, H. Fujisawa, M. Shimizu, Y. Haruyama, and H. Nishino, Light stability tests of CH 3 NH 3 PbI 3 perovskite solar cells using porous carbon counter electrodes. Phys. Chem. Chem. Phys. 18(39), (2016) 27102.
[6] A. Babayigit, A. Ethirajan, M. Muller, and B. Conings, Toxicity of organometal halide perovskite solar cells. Nat. Mater. 15(3), (2016) 247.
[7] S.F. Hoefler, G. Trimmel, and T. Rath, Progress on lead-free metal halide perovskites for photovoltaic applications: a review. Monatsh. Chem. 148(5), (2017) 795.
[8] C. Zhang, L. Gao, S. Hayase, and T. Ma, Current advancements in material research and techniques focusing on lead-free perovskite solar cells. Chem. Lett. 46(9), (2017) 1276.
[9] Y Y. Kim, Z. Yang, A. Jain, O. Voznyy, G.H. Kim, M. Liu, L. N. Quan, F.P. García de Arquer, R. Comin, J.Z. Fan, and E.H. Sargent, Pure Cubic-Phase Hybrid Iodobismuthates AgBi2I7 for Thin-Film Photovoltaics. Angew. Chem. 128(33), (2016) 9738.
[10] H. Zhu, D. Mingao Pan, M.B. Johansson, and E.M. Johansson, High Photon-to-Current Conversion in Solar Cells Based on Light-Absorbing Silver Bismuth Iodide. ChemSusChem 10(12), (2017) 2592.
[11] I. Turkevych, S. Kazaoui, E. Ito, T. Urano, K. Yamada, H. Tomiyasu, H. Yamagishi, M. Kondo, S. Aramaki, Photovoltaic Rudorffites: Lead-Free Silver Bismuth Halides Alternative to Hybrid Lead Halide Perovskites. ChemSusChem 10(19), (2017) 3754.
[12] K.W. Jung, M.R. Sohn, H.M. Lee, I.S. Yang, S. Do Sung, J. Kim, E.W-G Diau, and W.I. Lee, Silver bismuth iodides in various compositions as potential Pb-free light absorbers for hybrid solar cells. Sustainable Energy & Fuels 2(1), (2018) 294.
[13] Z. Shao, T. Le Mercier, M.B. Madec, and T. Pauporté, Exploring AgBixI3x+ 1 semiconductor thin films for lead-free perovskite solar cells. Mater. Des. 141, 81 (2018).
[14] Z. Shao, T. Le Mercier, M.B. Madec, and T. Pauporté, AgBi2I7 layers with controlled surface morphology for solar cells with improved charge collection. Mater. Lett. 221, (2018) 135.
[15] B. Ghosh, B. Wu, X. Guo, P.C. Harikesh, R.A. John, T. Baikie, Arramel, A.T. S. Wee, C. Guet, T. C. Sum, S. Mhaisalkar, and N. Mathews, Superior Performance of Silver Bismuth Iodide Photovoltaics Fabricated via Dynamic Hot-Casting Method under Ambient Conditions. Adv. Energy Mater. 8(33), (2018) 1802051.
[16] N. Pai, J. Lu, T.R. Gengenbach, A. Seeber, A.S. Chesman, L. Jiang, D.C. Senevirathna, P.C. Andrews, U. Bach, Y.B. Cheng, and A.N. Simonov, Silver bismuth sulfoiodide solar cells: tuning optoelectronic properties by sulfide modification for enhanced photovoltaic performance. Adv. Energy Mater. 9(5), (2019) 1803396.
[17] M. Khazaee, K. Sardashti, C.C. Chung, J.P. Sun, H. Zhou, E. Bergmann, W.A. Dunlap-Shohl, Q. Han, I.G. Hill, J.L. Jones, D.C. Lupascu, and D.B. Mitzi, Dual-source evaporation of silver bismuth iodide films for planar junction solar cells. J. Mater. Chem. A 7(5), (2019) 2095.
[18] S.S. Hosseini, and M. Adelifard, The Effect of Multi-walled Carbon Nanotubes and Reduced Graphene Oxide Doping on the Optical and Photovoltaic Performance of Ag 2 BiI 5-Based Solar Cells. J. Electron. Mater. 49(10), (2020) 5790.
[19] H. Zhu, J. Wei, K. Wang, and D. Wu, Applications of carbon materials in photovoltaic solar cells. Sol. Energy Mater. Sol. Cells 93(9), (2009) 1461.
[20] S.N. Habisreutinger, T. Leijtens, G.E. Eperon, S.D. Stranks, R.J. Nicholas, and H.J. Snaith, Carbon nanotube/polymer composites as a highly stable hole collection layer in perovskite solar cells. Nano Lett. 14(10), (2014) 5561.
[21] Z. Wei, H. Chen, K. Yan, X. Zheng, and S. Yang, Hysteresis-free multi-walled carbon nanotube-based perovskite solar cells with a high fill factor. J. Mater. Chem. A 3(48), (2015) 24226.
[22] K. Aitola, K. Sveinbjörnsson, J.P. Correa-Baena, A. Kaskela, A. Abate, Y. Tian, E.M.J. Johansson, M. Grätzel, E.I. Kauppinen, A. Hagfeldt, and G. Boschloo, Carbon nanotube-based hybrid hole-transporting material and selective contact for high efficiency perovskite solar cells. Energy Environ. Sci. 9(2), (2016) 461.
[23] K. Aitola, K. Domanski, J.P. Correa-Baena, K. Sveinbjörnsson, M. Saliba, A. Abate, M. Grätzel, E. Kauppinen, E.M.J. Johansson, W. Tress, A. Hagfeldt, and G. Boschloo, High temperature-stable perovskite solar cell based on low-cost carbon nanotube hole contact. Adv. Mater. 29(17), (2017) 1606398.
[24] Q. Luo, Y. Zhang, C. Liu, J. Li, N. Wang, and H. Lin, Iodide-reduced graphene oxide with dopant-free spiro-OMeTAD for ambient stable and high-efficiency perovskite solar cells. J. Mater. Chem. A 3(31), (2015) 15996.
[25] A.L. Palma, L. Cinà, S. Pescetelli, A. Agresti, M. Raggio, R. Paolesse, F. Bonaccorso, and A. Di Carlo, Reduced graphene oxide as efficient and stable hole transporting material in mesoscopic perovskite solar cells. Nano Energy 22, (2016) 349.
[26] M.M. Tavakoli, R. Tavakoli, Z. Nourbakhsh, A. Waleed, U.S. Virk, and Z. Fan, High efficiency and stable perovskite solar cell using ZnO/rGO QDs as an electron transfer layer. Adv. Mater. Interfaces 3(11), (2016) 1500790.
[27] S.S. Mali, C.S. Shim, H. Kim, and C.K. Hong, Reduced graphene oxide (rGO) grafted zinc stannate (Zn 2 SnO 4) nanofiber scaffolds for highly efficient mixed-halide perovskite solar cells. J. Mater. Chem. A 4(31), (2016) 12158.
[28] E. Nouri, M.R. Mohammadi, Z.X. Xu, V. Dracopoulos, and P. Lianos, Improvement of the photovoltaic parameters of

perovskite solar cells using a reduced-graphene-oxide-modified titania layer and soluble copper phthalocyanine as a hole transporter. Phys. Chem. Chem. Phys. 20(4), (2018) 2388.